EFFECT OF ORIENTATIONAL ORDER ON THE DECAY OF THE FLUORESCENCE ANISOTROPY IN MEMBRANE SUSPENSIONS

Experimental Verification on Unilamellar Vesicles and Lipid/α-Lactalbumin Complexes

MARCEL AMELOOT AND HUBERT HENDRICKX
Limburgs Universitair Centrum, Division of Biophysics, Universitaire Campus, B-3610 Diepenbeek, Belgium

WILLY HERREMAN, HANS POTTEL, AND FRANS VAN CAUWELAERT
Interdisciplinair Research Centrum, Katholieke Universiteit Leuven, Campus Kortrijk, B-8500 Kortrijk, Belgium

WIEB VAN DER MEER
Physiological Laboratory, University of Leiden, NL-2300 RC Leiden, The Netherlands

ABSTRACT Various models for the analysis of time-dependent fluorescence anisotropy measurements were evaluated. The discussion was based on the analysis of pulsed experiments with 1,6-diphenyl-1,3,5-hexatriene embedded in small unilamellar vesicles of dimyristoylphosphatidylcholine or dipalmitoylphosphatidylcholine and in dimyristoylphosphatidylcholine/α-lactalbumin complexes. It was shown that a recently proposed model (Van der Meer, W., H. Pottel, W. Herreman, M. Ameloot, H. Hendrickx, H. Schröder, 1984, *Biophys. J.*, 46:515–523) described the data better than did the earlier suggested cone model (Kinosita K., Jr., S. Kawato, and A. Ikegami, 1977, *Biophys. J.*, 20:289–305). This permitted the use of the new model for the estimation of the second- and fourth-rank order parameters on nonoriented systems. The results indicated that a fraction of the probes was oriented perpendicularly to the preferred direction of the lipids. An increase of the rotational correlation times of the fluorescent probe and a higher order of its environment were detected after the interaction of α-lactalbumin with the dimyristoylphosphatidylcholine vesicles at acidic pH at 24.2°C.

INTRODUCTION

Fluorescent probing of membrane vesicles has been widely applicated. The use of the easy and rapid steady state anisotropy method has provided a wealth of experimental data. However, the more laborious time-dependent anisotropy measurements were necessary to clarify the meaning of the results obtained under steady state conditions. The most important point is that the fluorescence anisotropy of most probes is found not to relax to zero value (1–4). This indicates that the motion of the probe is restricted by the surrounding structure. Consequently, time-dependent anisotropy measurements may provide structural and dynamic information (5–7).

Various experimental methods and models have been suggested to extract this information from the experimental data. This paper reviews the data analysis for pulsed systems and compares the different models on the same real data sets. The behavior of the fluorescent probe 1,6-diphenyl-1,3,5-hexatriene (DPH) in vesicles of dimyristoylphosphatidylcholine (DMPC) or dipalmitoylphosphatidylcholine (DPPC) will be reexamined. The experimental data for the discussed systems are always better described by a recently proposed model (8) than by the earlier suggested cone model (5, 9, 10). The discrepancy is most pronounced above the transition temperature of the vesicle system. The estimated distribution function then deviates considerably from the cone distribution and it

Dr. Ameloot's present address is the Department of Biology, Johns Hopkins University, Baltimore, Maryland 21213.
W. van der Meer's current address is Division of Cell Biology, Antoni van Leeuwenhoekhuis, The Netherlands Cancer Institute, 121 Plesmanlaan, 1066 CX Amsterdam, The Netherlands.

Address all correspondence to Dr. W. Herreman.

exhibits a secondary maximum in the direction perpendicular to the membrane normal. This second maximum is not found for 1-[4-(trimethylamino)phenyl]-6-phenyl-1,3,5-hexatriene (TMA-DPH), a cationic analogue of DPH.

Original time-dependent anisotropy measurements for DPH embedded in the DMPC/α-lactalbumin complex at pH 4 and 24.2°C are presented. The conclusions concerning the various anisotropy models are similar to those for the pure lipid vesicles. In the complex the second- and fourth-order parameters have high values that are comparable to those found for the pure lipid vesicles below the transition temperature (T_c).

THE DECONVOLUTION PROBLEM AND FITTING PROCEDURES

The time-dependent fluorescence anisotropy $r(t)$ is given by

$$r(t) = \frac{i_\parallel(t) - i_\perp(t)}{i_\parallel(t) + 2\, i_\perp(t)}, \tag{1}$$

where $i_\parallel(t)$ and $i_\perp(t)$ denote the fluorescence intensities in the parallel and perpendicular direction with respect to the polarization of the excitation light. The latter is assumed to be vertically oriented on the excitation-emission plane. When a pulsed system is used (e.g., reference 11) the observed polarized fluorescence intensities, $I_\parallel(t)$ and $I_\perp(t)$, are convolution products of the measured excitation profile $L(t)$ with the δ-pulse responses $i_\parallel(t)$ and $i_\perp(t)$, i.e.,

$$I_\parallel(t) = \int_0^t L(u)\, i_\parallel(t-u)\, du \equiv i_\parallel(t) * L(t) \tag{2a}$$

$$I_\perp(t) = \int_0^t L(u)\, i_\perp(t-u)\, du \equiv i_\perp(t) * L(t). \tag{2b}$$

It will be assumed that the observed polarization components are corrected for polarization bias and wavelength dependence in the detection (e.g., reference 11).

Denoting the intrinsic fluorescence relaxation by $s(t)$, the following relations will hold for the usual 90° geometry of excitation detection:

$$s(t) = i_\parallel(t) + 2\, i_\perp(t) \tag{3a}$$

$$i_\parallel(t) = \frac{s(t)}{3}\,[1 + 2r(t)] \tag{3b}$$

$$i_\perp(t) = \frac{s(t)}{3}\,[1 - r(t)]. \tag{3c}$$

In most cases $s(t)$ can be written as

$$s(t) = \sum_{i=1}^{n} a_i \exp(-t/\tau_i). \tag{4}$$

It is reasonable to assume that the anisotropy $r(t)$ in membranes can be approximated by a sum of a limited number of exponential relaxations and a constant

$$r(t) = \sum_{j=1}^{m} b_j \exp(-t/\phi_j) + b_{m+1}, \tag{5}$$

where b_{m+1} stands for $r(\infty)$. Note that, in contrast to $\{a_i\}$, the preexponential factors $\{b_i\}$ are absolute. The value at zero time, $r(0) = \sum_{j=1}^{m+1} b_j$, will be called the fundamental anisotropy of the probe and is denoted by r_0.

A commonly used method for the determination of the sets $\{a_i, \tau_i\}$ and $\{b_j, \phi_j\}$ is the following. The total fluorescence decay $s(t)$ is recovered from

$$S(t) = I_\parallel(t) + 2\, I_\perp(t) = s(t) * L(t) \tag{6}$$

by a deconvolution procedure. This problem has been treated in a number of papers and meetings (12, 13) and will not be discussed here in detail. A difference curve $D(t)$ is then constructed from the experimental decays

$$\begin{aligned} D(t) &= I_\parallel(t) - I_\perp(t) \\ &= [i_\parallel(t) - i_\perp(t)] * L(t) \equiv d(t) * L(t). \end{aligned} \tag{7}$$

In the case of rotational homogeneity (3) $d(t)$ will be given by

$$d(t) = r(t)\, s(t). \tag{8}$$

The parameters of the anisotropy $\{b_j, \phi_j\}$ are then obtained by repeating the deconvolution on $D(t)$ and by fixing the recovered parameter values for $\{a_i, \tau_i\}$.

The nonlinear least-squares search is recommended for this purpose because it recovers the parameters very well and because it provides a number of worthwhile evaluation criteria and parameter statistics (e.g., reference 14). The correct statistical weights then have to be used for the constructed sum and difference curve (15). However, it has been found that equal weighting leads to a better recovery of the anisotropy parameters from the difference curve $D(t)$ (3).

The problem of choosing the correct weights can be circumvented by applying the vector analysis that has been suggested by C. W. Gilbert and communicated by Dale (16). In this method the two polarization components are considered simultaneously in a single deconvolution step. The natural weighting (Gaussian or Poissonian) can then be used and the usual evaluation criteria can be maintained.

In the case in which all parameters are freely adjustable, large uncertainties may result on the resulting values for the more elaborate descriptions of the time-dependent anisotropy. To reduce the number of free parameters, the fundamental anisotropy may be fixed in the analysis (17). Another combination method has been suggested that eliminates the need for the matching factor between the polarization components (18). This approach, based on the Laplace transform method, seems to be restricted to simple systems.

Recently, André et al. (19) described a numerical deconvolution method yielding the $r(t)$ curve without assuming explicit expressions. This method has much to be recommended. However, we preferred to compare the

TABLE I
MODELS FOR THE TIME-DEPENDENT FLUORESCENCE ANISOTROPY

Number of exponentials	Notation	Description	References
1	r_{c1}	Cone model	5, 9
	r_{g1}	General model	8, 9, 17
2	r_{m2}	Purely mathematical	3
3	r_{c3}	Cone model	10
	r_{g3}	General model	8
	r_{gc}	r_{g3} Specified for cone	8

different physical models for the anisotropy on the basis of the quality of the fit to the original data.

SURVEY OF THE ANISOTROPY MODELS

The notations for the different expressions of the fluorescence anisotropy discussed in this paper are listed in Table I. It will be assumed that the probe DPH behaves as a stiff rod and that at least one of the optical transition moments lies along the symmetry axis. The orientation distribution function of the probe can be taken to be axially symmetric around the normal to the membrane surface. This function will then depend only on the angle θ between the probe axis and the normal. In that case the ratio $r(\infty)/r(0)$ is equal to the square of the second-rank order parameter $\langle P_2 \rangle$, i.e., the ensemble average of the second Legendre polynomial (see Appendix A) (6, 7).

In the last years, much attention has been paid to a theoretical description of the dynamics of rotational motion in an anisotropic environment (20). The rotational diffusion model is usually adopted. Within this framework, the diffusion coefficient $D_\perp$ for the rotation around an axis perpendicular to the symmetry axis of the probe can be estimated for a rodlike probe from the initial slope of $r(t)$ (5),

$$D_\perp = -\frac{1}{6r_0}\frac{\partial r}{\partial t}\bigg|_{t=0}. \tag{9}$$

According to the mathematical description of the anisotropy in Eq. 5, this results in

$$D_\perp = \frac{1}{6\,r_0}\sum_{j=1}^{m}\frac{b_j}{\phi_j}. \tag{10}$$

The latter is merely an extension of an earlier suggested model-independent interpolation, which is here denoted by r_{g1} (8, 9, 17)

$$r_{g1}(t) = [r(0) - r(\infty)]\exp(-t/\phi) + r(\infty), \tag{11}$$

with

$$\phi = (1 - \langle P_2 \rangle^2)/6D_\perp. \tag{12}$$

The behavior of $r(t)$ at intermediate times can be estimated from a more elaborated physical model. One may assume that the effect of the environment on the probe can be described by taking an effective reorienting potential. The corresponding Smoluchowski equation (see e.g. reference 8) has then to be solved.

A simple model has been proposed in which the symmetry axis of the probe wobbles uniformly within a cone of semiangle θ_c (5). The solution of the diffusion equation for this potential cannot be written in closed form. Hence the resulting expressions are suited for the analysis of experimental data. Approximations have been proposed that share some properties with the exact solution.

A single exponential approximation, to be referenced as $r_{c1}(t)$, with the same area under the curve as was seen with the exact solution has been suggested (5, 9). The relaxation time ϕ in Eq. 11 then has to be replaced (9) by

$$\phi = (A + B)/[D_\perp(1 - \langle P_2 \rangle^2)], \tag{13}$$

with

$$A = -x_c^2(1 + x_c)^2\{\ln[(1 + x_c)/2] + (1 - x_c)/2\}/[2(1 - x_c)],$$

$$B = (1 - x_c)(6 + 8x_c - x_c^2 - 12x_c^3 - 7x_c^4)/24,$$

$$x_c = \cos\theta_c.$$

TABLE II
EXPRESSIONS FOR THE CONE MODEL* $r_{c3}(t) = \Sigma_{j=1}^{3} b_j \exp(-t/\theta_j) + b_4$, $(x = \cos\theta_c)$

j	b_j	ϕ_j
1	$\frac{r_0}{20}[x(1 + x)(9x^2 - 1) + 4] - r_0\left[\frac{1}{2}x(1 + x)\right]^2$	$\frac{r_0}{D_\perp b_1}\left[\frac{x^2(1 + x)^2}{2(x - 1)}\left(\ln\frac{1 + x}{2} + \frac{1 - x}{2}\right) + (1 - x)(2 - x - 9x^2 - 7x^3)/60\right]$
2	$\frac{r_0}{5}(1 - x)[(2 + x)(1 + 3x^2) + 3x]$	$\frac{r_0}{60D_\perp b_2}(1 - x)^2(9 + 32x + 44x^2 + 20x^3)$
3	$\frac{r_0}{20}(1 - x)^2(3x^2 + 9x + 8)$	$\frac{r_0}{120\,D_\perp b_3}(1 - x)^3(8 + 12x + 5x^2)$
4	$r_0[\frac{1}{2}x(1 + x)]^2$	—

*See reference 10.

From the graphical comparison with the exact numerical solution (5) one can expect that, at least for larger cone angles, this will be a poor approximation. A more accurate expression may be obtained in the following way.

It has been shown that the anisotropy can be decomposed as a sum of rotational correlation functions (see references 8, 10 and Appendix B) G_{k0}

$$r(t)/r(0) = \sum_{k=-2}^{k=+2} G_{k0}(t), \tag{14}$$

where

$$G_{k0}(t) = G_{-k0}(t).$$

Requiring that each correlation function has the exact area, Lipari and Szabo (10) suggest a triple exponential approximation denoted here by $r_{c3}(t)$. The corresponding preexponentials and relaxation constants are given in Table II.

A more realistic harmoniclike potential may be considered (17). This leads to a distribution function of the Gaussian type

$$f(\theta) \sim \exp(-\cos^2\theta/2\sigma^2), \tag{15}$$

where σ specifies the width of the distribution. The exact solution of the diffusion equation for this potential has been discussed by Nordio and Segre (21). An infinite number of exponential functions is obtained for each correlation function. By retaining only the leading term a triple exponential expression for $r(t)$ is achieved for the assumed symmetry of the probe.

Note that the mentioned cone and Gaussian distribution are both completely characterized by $\langle P_2 \rangle$. The cone angle may be estimated from (5)

$$\frac{r(\infty)}{r(0)} = \langle P_2 \rangle^2 = \left[\frac{1}{2}\cos\theta_c\,(1 + \cos\theta_c)\right]^2. \tag{16}$$

Numerical integration is required for the determination of the parameter σ of the Gaussian distribution.

The question arises then whether these triple exponential approximations offer a great advantage for distributions that are completely characterized by $\langle P_2 \rangle$. This parameter may also be estimated from a data analysis using a pure mathematical description: an expression with two exponential relaxations and a constant (3). This approach will be indicated by $r_{m2}(t)$. Because the parameters in $r_{m2}(t)$ are independent of each other, this expression may describe a wide variety of anisotropy decays. Therefore, it may be expected that the value of the diffusion coefficient $D_\perp$ calculated from Eq. 10 will be reliable.

In a preceding paper, an approximate solution of the Smoluchowski equation has been suggested without specifying the type of potential beforehand (8). In this sense, the new description may be called general and is denoted by $r_{g3}(t)$. Each correlation function $G_{k0}(t)$ is approximated by a single exponential expression, which has the correct slope at zero time. The anisotropy r_{g3} is then expressed in terms of $D_\perp$ and the order parameters $\langle P_2 \rangle$ and $\langle P_4 \rangle$ (see Table III). A further generalization could be obtained by considering that the relaxation times ϕ_j are independent. However, very large standard deviations then result.

The general approach can be specified towards a particular distribution by introducing the corresponding averages $\langle P_2 \rangle$ and $\langle P_4 \rangle$ in the expressions of $r_{g3}(t)$. For example, when the order parameters of the cone model (see Appendix A) are used, an alternative triple exponential approximation is obtained for this model, $r_{gc}(t)$. The preexponential factors of $r_{gc}(t)$ are those of $r_{c3}(t)$ but the relaxation constants are different.

MATERIALS AND METHODS

Materials

DPH, DMPC, DPPC, and α-lactalbumin from bovine milk were obtained from Sigma Chemical Corp. (St. Louis, MO) and were used as supplied. The purity of DPH was verified on high pressure liquid chromatography. The fluorescent probe TMA-DPH was purchased from Molecular Probes (Plane, TX). All other materials were of spectroscopic or analytical grade.

Preparations

Single-walled bilayer vesicles were prepared essentially as described by Chen et al. (2). The required amount of lipid was dissolved in chloroform

TABLE III

EXPRESSIONS FOR THE GENERAL MODEL* $r_{g3}(t) = \Sigma_{j=1}^{3} b_j \exp(-t/\theta_j) + b_4$

j	b_j	ϕ_j
1	$r_0(1/5 + 2\langle P_2\rangle/7 + 18\langle P_4\rangle/35 - \langle P_2\rangle^2)$	$\frac{b_1}{6r_0 D_\perp}(1/5 + \langle P_2\rangle/7 - 12\langle P_4\rangle/35)^{-1}$
2	$2r_0(1/5 + \langle P_2\rangle/7 - 12\langle P_4\rangle/35)$	$\frac{b_2}{6r_0 D_\perp}(1/5 + \langle P_2\rangle/14 + 8\langle P_4\rangle/35)^{-1}$
3	$2r_0(1/5 - 2\langle P_2\rangle/7 + 3\langle P_4\rangle/35)$	$\frac{b_3}{12r_0 D_\perp}(1/5 - \langle P_2\rangle/7 - 2\langle P_4\rangle/35)^{-1}$
4	$r_0\langle P_2\rangle^2$	—

*See reference 8.

in a round bottomed 5-ml flask. DPH in chloroform was then added to assure a probe/lipid ratio of 1:500. After the evaporation step, a 4-ml buffer (0.1 M in NaCl and 10 mM in TRIS [pH 7.4] or 10 mM in acetate [pH 4]) was added. The mixture was then sonicated for 1 h in a water bath at ±42° C with a MSE Scientific Instruments (Manor Royal, Crawley, Sussex, England) sonicator at the 9 μm level using the exponential probe. The sample volume was made up to 6 ml and centrifuged in a Beckman (type L5-65; Beckman Instruments, Geneva, Switzerland), with a preheated aluminium n° 40 rotor at 40,000 rpm for 1 h. The measurements were performed on the supernatant. A final concentration of ~0.8 mg lipid/ml was obtained. The preparations were never heated from below the transition temperature of the system. α-Lactalbumin solutions with a concentration of 24 mg/ml were made in bidistilled water. Different amounts of the α-lactalbumin solution were added to 3 ml of the vesicle suspension. The measurements on the lipid-protein complexes were made the protein was incubated with DMPC for 20 h at 24°C. Protein concentrations in the complex were determined by the fluorescamine method of Böhlen et al. (22). Phospholipid analysis is based on the formation of phosphomolybdenum blue, using the procedure of Vaskovsky et al. (23).

Instruments

The time-dependent fluorescence anisotropy was measured on a computer controlled single photon counting apparatus. The optical part and the detector (Mullard 56 DUVP/03) were purchased from Applied Photophysics Ltd. (London, England). The thyratron-gated flashlamp was filled with air and operated at 18 kHz. The electronic modules were delivered by Canberra Industries (Meriden, CT) and Ortec (Oak Ridge, TN). The multichannel analyzer S-80 from Canberra Industries was connected directly to a PDP 11/34 (Digital Equipment Corp., Malboro, MA) allowing for the interrupt facility. Instabilities of the gated nanosecond flashlamp were eliminated by measuring the two polarization components and the excitation profile in an alternating way (24). The latter was recorded at the excitation wavelength (358 nm) using the suspension as a scatterer. Monochromators were used in the excitation and in the emission path as well. The motors of the polarization unit and of the emission monochromator were controlled by the computer interfaced by a CAMAC-module of Kinetic Systems Corp. (Lockport, IL). The excitation light was vertically polarized. Both polarizers were Polaroid HNP'B (Polaroid Corp., Cambridge, MA). The polarization bias γ was determined as described by Chen and Bowman (25). Steady state anisotropies were measured with the same apparatus by using the multichannel analyzer in multiscaling mode and by repetitive switching of the emission polarizers.

Data Analysis (General Remarks)

The deconvolution was carried out according to the vector analysis (16). The parameters were determined by the iterative reconvolution method (26) using the nonlinear least squares algorithm due to Marquardt (27). The statistical weights were chosen in accordance to photon counting error. The convolution products were calculated by the procedures suggested by Grinvald (26, 28). Only the channels with a reasonable amount of counts (≥100) were considered in the analyses. The quality of the fit was judged by the statistics of the weighted residuals between the observed and the calculated value (14, and references therein). More specifically, the reduced chi square χ_r^2 (29) as applied to the vector analysis is defined as

$$\chi_r^2 = \frac{1}{2(N_2 - N_1 + 1) - n} \sum_{i=N_1}^{N_2} \left\{ \frac{(I_{\parallel}^0 - I_{\parallel}^c)^2}{I_{\parallel i}^0} + \frac{(I_{\perp i}^0 - \gamma I_{\perp i}^c)^2}{I_{\perp i}^0} \right\}. \quad (17)$$

The observed and the calculated intensities are denoted, respectively, by the superscripts (^{0}) and (^{c}); N_1 and N_2 correspond, respectively, to the first and the last channel considered in the analysis; n is the number of parameters that are freely adjustable. For the considered degrees of freedom, the critical value of χ_r^2 is given by $\chi_r^2 \simeq 1.11$ at the 0.05 significance level. Because the statistics are influenced by the total number of the collected counts in the multichannel analyzer, all data sets were collected for about the same number of counts (≈25,000 counts in the peak of the parallel polarization component). Some prolonged experiments were performed also. To reduce the number of the independent parameters the time-shift between the measured excitation profile and the polarization components was determined for each experiment from a preceding analysis of the total fluorescence.

THE TIME-DEPENDENT FLUORESCENCE ANISOTROPY OF DPH IN SONICATED VEISCLES

Results

Time-dependent anisotropy measurements were performed on DPH-doped unilamellar vesicles of DMPC or DPPC at various temperatures. Satisfiable fits of the total fluorescence decay, measured under magic angle conditions (see, e.g., reference 11) or constructed from the two polarization components, were obtained only when two relaxation constants were considered. This agrees with previous reports (2, 3, 30). The parameters for the total fluorescence decay are given in Table IV. Above the transition temperature of the system the fractional amplitude of the short-living component is ~15% and increases

TABLE IV
THE DECAY PARAMETERS FOR THE TOTAL FLUORESCENCE EMISSION, $s(t)$, OF DPH IN UNILAMELLAR VESICLES OF DMPC AND DPPC
$s(t) = \Sigma_{i=1}^{2} a_i \exp(-t/\tau_i)$

Sample	T(°C)	a_1	a_2	τ_1	τ_2
				ns	*ns*
DMPC	7.7	0.39	0.61	4.6	10.01
		(0.02)*	(0.02)	(0.1)	(0.07)
	16.3	0.28	0.72	6.0	11.3
		(0.04)	(0.04)	(0.4)	(0.1)
	24.3	0.227	0.773	2.4	9.30
		(0.006)	(0.006)	(0.1)	(0.03)
	35.4	0.138	0.862	3.4	8.34
		(0.009)	(0.009)	(0.2)	(0.03)
	42.0	0.142	0.858	3.2	7.77
		(0.009)	(0.009)	(0.2)	(0.03)
DPPC	22.3	0.27	0.73	4.6	10.12
		(0.02)	(0.02)	(0.2)	(0.07)
	32.4	0.27	0.73	4.1	9.98
		(0.01)	(0.01)	(0.2)	(0.06)
	40.3	0.17	0.83	3.6	8.70
		(0.01)	(0.01)	(0.3)	(0.04)
	45.4	0.14	0.86	3.1	8.06
		(0.01)	(0.01)	(0.3)	(0.03)
	51.8	0.158	0.842	2.2	7.76
		(0.006)	(0.006)	(0.2)	(0.02)

*Standard deviations are denoted within parentheses.

as temperature is lowered. The origin of this biexponential behavior is still an open question (3). However, it has been found that the average lifetime shows a remarkable correlation with order (31, 32, 33). Because all parameters are adjusted simultaneously during the least-squares search, the estimates of the parameters of the fluorescence, $s(t)$, and the anisotropy $r(t)$ will be correlated. However, we found that the correlation is not so strong. The fluorescence parameters resulting from the different analyses are quite comparable, except for the single exponential descriptions r_{c1} and r_{g1}.

By using the mentioned vector procedure, the measurements were analyzed according to the approaches given in Table I. Two relaxations in the total fluorescence and rotational homogeneity (3) were assumed throughout. The value of the fundamental anisotropy r_0 was kept fixed to a predetermined value, $r_0 = 0.380$. Several arguments can be given for that. The determination of r_0 from a time-resolved experiment on vesicles seems to be difficult. Large uncertainties on the other anisotropy parameters result for the more elaborated models if r_0 is a freely adjustable parameter. Kinosita et al. (17) argued that if r_0 is let free in the curve fitting, r_0 tends to be underestimated. Using synchroton radiation as an excitation source, Wolber et al. (34) concluded that some of the anisotropic decays are too fast to be detected so that a lower r_0 will be calculated. Different values for r_0 of the DPH probe when excited at ± 355 nm in isotropic rigid media are given in the literature (0.362–0.395) (1, 3, 35, 36). Somewhat lower values are reported for vesicles of DMPC (0.296–0.338) (2) and egg lecithin (0.307–0.358) (3). This lower value may be explained by depolarizing effects in the vesicle systems (3). We determined r_0 from the limiting steady state anisotropy r_s obtained by cooling a glycerin solution. A value of 0.380 ± 0.001 was obtained, which compares very well with the reported value of 0.378 in polyisobutylene (36). The effect of fixing r_0 at a certain value on the resulting parameter values will be discussed further on.

The reduced chi square value χ_r^2 for the different analyses for the DMPC and DPPC vesicles are given in Table V. Note that these values have been corrected for the polarization bias γ in the detection. At all temperatures, the best fits are obtained for r_{m2} and r_{g3}. Both descriptions yield practically the same low value of χ_r^2. The χ_r^2 values for the models r_{c3} and r_{gc} are very similar but higher. Below the transition temperature of the system, the quality of the fits for the mono-exponentials is comparable with those obtained for the cone model r_{c3} and r_{gc}. Above the transition temperature, a single exponential becomes really inadequate and also the cone models fail. When the total number of collected counts is increased in a prolonged experiment, the discrepancy between the various descriptions becomes more pronounced; a visual interpretation of the sequence of the weighted residuals and their autocorrelation may then indicate the best description of the data.

TABLE V

THE QUALITY OF THE FITS AS JUDGED BY THE REDUCED CHI SQUARE VALUE, χ_r^2,* ACCORDING TO THE VARIOUS DESCRIPTIONS OF THE FLUORESCENCE ANISOTROPY FOR DPH IN UNILAMELLAR VESICLES OF DMPC AND DPPC

Sample	T(°C)	r_{c1} / r_{g1}	r_{c3}	r_{gc}	r_{g3}	r_{m2}
DMPC	7.7	1.33	1.31	1.31	1.15	1.15
	16.3	1.37	1.35	1.35	1.17	1.14
	24.3	1.66	1.46	1.43	1.16	1.15
	35.4	2.16	1.50	1.58	1.01	1.02
	42.0	2.12	1.59	1.73	1.27	1.28
DPPC	22.3	1.26	1.25	1.25	1.15	1.15
	32.4	1.23	1.21	1.21	1.10	1.09
	40.3	1.65	1.40	1.38	1.11	1.11
	45.4	1.75	1.44	1.45	1.12	1.11
	51.8	1.63	1.42	1.46	1.24	1.24

*See Eq. 17.

When the number of counts is doubled, we found for DMPC at 35.4°C the following χ_r^2 values

model:	χ_r^2:
r_{g1}, r_{c1}	3.08
r_{gc}	2.08
r_{c3}	1.92
r_{m2}	1.11
r_{g3}	1.09.

The two polarization components of this experiment are represented in Fig. 1 *A* and *B*. The weighted residuals and their autocorrelation are shown for r_{g3} (Fig. 1 *C* and *D*) and r_{c3} (Fig. 1 *E*, *F*). It can be concluded from visual inspection that r_{g3} has to be favored. The large residuals for the r_{c3} model in the first channels are characteristic and confirm the importance of considering the raising edge in the analysis (14). The same profile is obtained for the r_{gc} description. This means that the nature of the approximation (correct area for r_{c3}, correct slope at zero time for r_{gc}) is not of particular importance. This also implies the inadequacy of the cone model. It is also possible to calculate χ_r^2 for each polarization component separately. Although both values improve significantly from r_{c3} towards r_{g3}, the biggest change can be noted for the perpendicular component.

The relaxation times ϕ_j in the anisotropy corresponding to the models r_{m2}, r_{c3}, and r_{g3} are represented in Fig. 2 *A*, *B*. The results for both lipid systems are quite similar. The relaxation times of r_{c3} are practically constant. In contrast, the relaxation times in r_{g3} and the largest one in r_{m2} show a temperature dependence. The largest relaxation times in r_{g3} and r_{m2} are nearly equal and reach rather high values at $T < T_c$. So, the highest relaxation times in r_{c3} and r_{g3}, which also have the largest preexponential factors, are signifi-

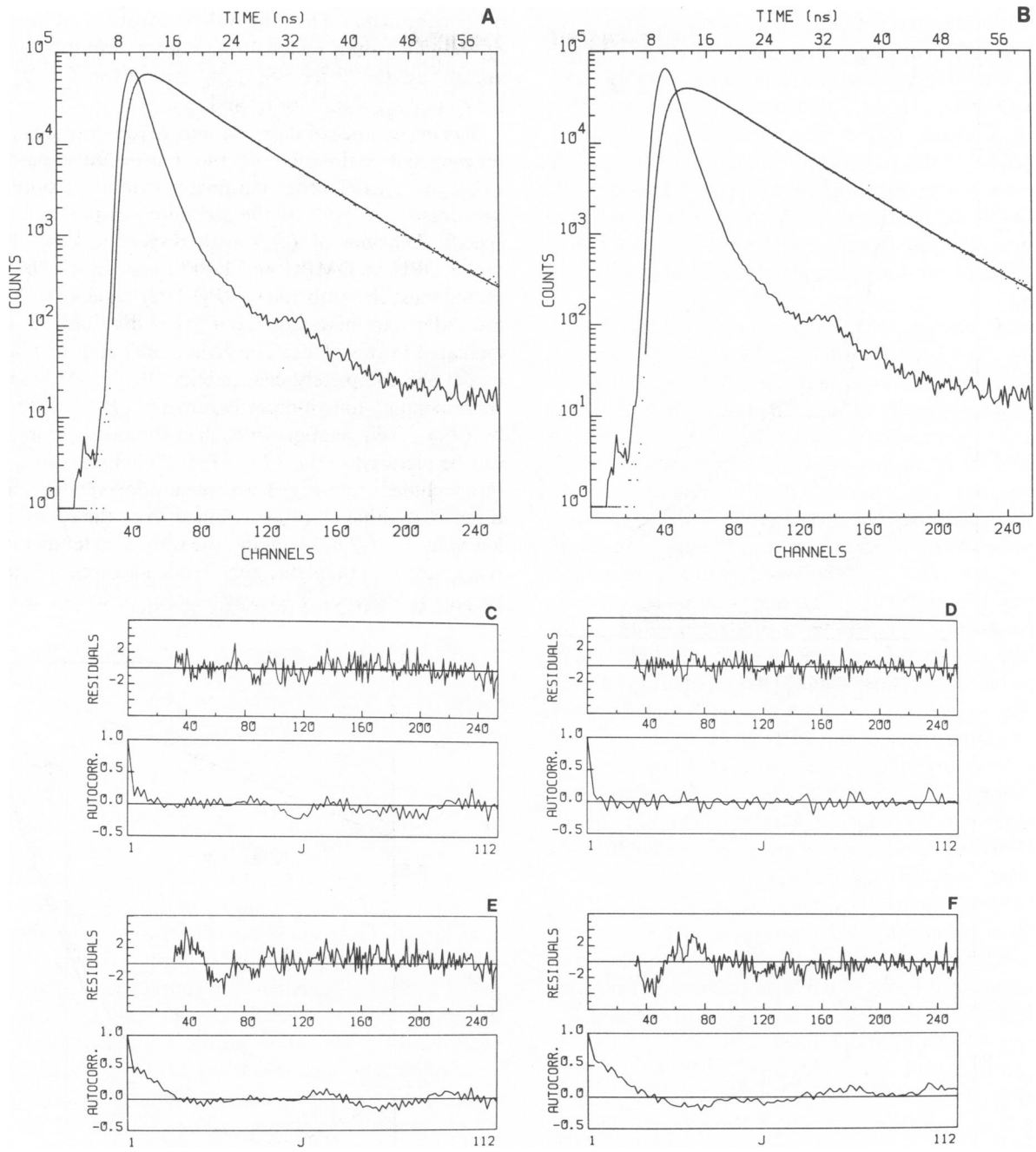

FIGURE 1 Time-dependent fluorescence anisotropy experiment of DPH embedded in DMPC vesicles at 35.4°C. The polarized decay curves $I_{\parallel}(t)$ and $I_{\perp}(t)$ are represented, respectively, in *A* and *B*. The dots indicate the experimental points and the solid lines represent the measured excitation profile and the fitting curve calculated according to the general anisotropy model $r_{g3}(t)$. The weighted residuals and their autocorrelation according to $r_{g3}(t)$ are shown in *C* for $I_{\parallel}(t)$ and in *D* for $I_{\perp}(t)$. The corresponding curves of the weighted residuals according to the cone model $r_{c3}(t)$ are given in *E* for $I_{\parallel}(t)$ and in *F* for $I_{\perp}(t)$. *Autocorr.*, autocorrelation.

cantly different below T_c. The smallest relaxation times of r_{c3} are almost equal and have the value of the second relaxation in r_{m2}. These relaxation times lie practically between the two smallest relaxation times of r_{g3}.

An attempt has been made to analyze the data by considering an expression for the anisotropy with three freely adjustable relaxation times, ϕ_j. The preexponential factors were those of r_{g3} because of their general validity. Although the resulting relaxation times, ϕ_j, suffered from rather large uncertainties, they showed the same behavior as those of r_{g3}.

The limiting anisotropy $r(\infty)$ is model independent. However, its value depends on the specific expression used in the fitting procedure because of the correlation with the

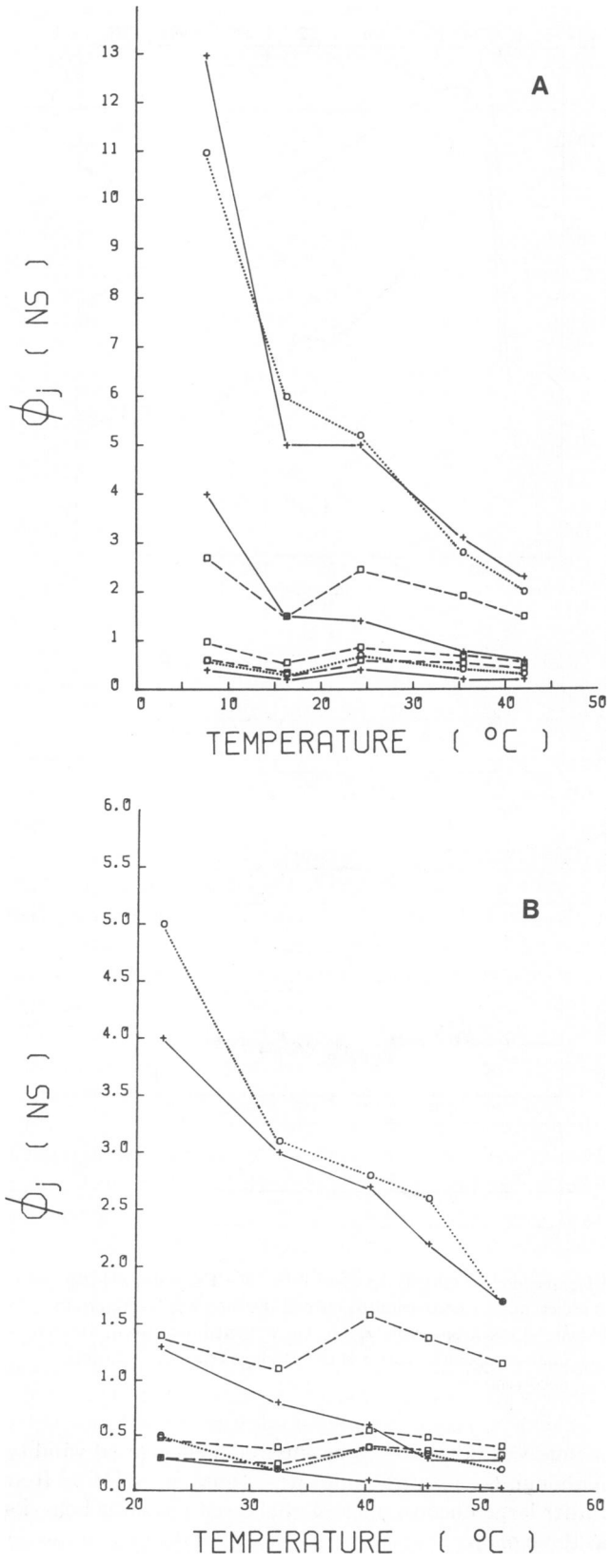

FIGURE 2 The relaxation times ϕ_j in the expressions of the fluorescence anisotropy according to the descriptions $r_{m2}(t)$ (· O ·) $r_{c3}(t)$ (—□—) and $r_{g3}(t)$ (—+—) as obtained from the experiments on DPH in vesicles of (*A*) DMPC and (*B*) DPPC.

other parameters. The same values are obtained for r_{m2} and r_{g3}. Higher values result for the other descriptions of the anisotropy, the difference being largest for $T > T_c$ (≈7% for r_{c3} and r_{gc}, ≈10% for r_{c1} and r_{g1}).

The importance of the more general description r_{g3} is the independent estimation of the fourth-order parameter $\langle P_4 \rangle$. At T_c, this order parameter exhibits a similar but less drastic behavior as the second-order parameter. The specific behavior of $\langle P_4 \rangle$ with respect to $\langle P_2 \rangle$ for the probe DPH in DMPC and DPPC vesicles can be represented most elegantly in the $\langle P_2 \rangle \langle P_4 \rangle$ plane (Fig. 3). Also the order parameters of the a priori distributions can be indicated in this plane. The cone model and the Gaussian model are completely characterized by $\langle P_2 \rangle$. Hence the corresponding fourth-order parameter $\langle P_4 \rangle$ is determined by $\langle P_2 \rangle$. Their relation for each of the two a priori models can be pictured in the $\langle P_2 \rangle \langle P_4 \rangle$ plane by a curve. It can be concluded from Fig. 3 that the a priori models underestimate the value of $\langle P_4 \rangle$ obtained from the r_{g3} model. At low values of $\langle P_2 \rangle$, i.e., above the transition temperature of the systems, totally different tendencies result from the various approaches. This is also indicated by the increment

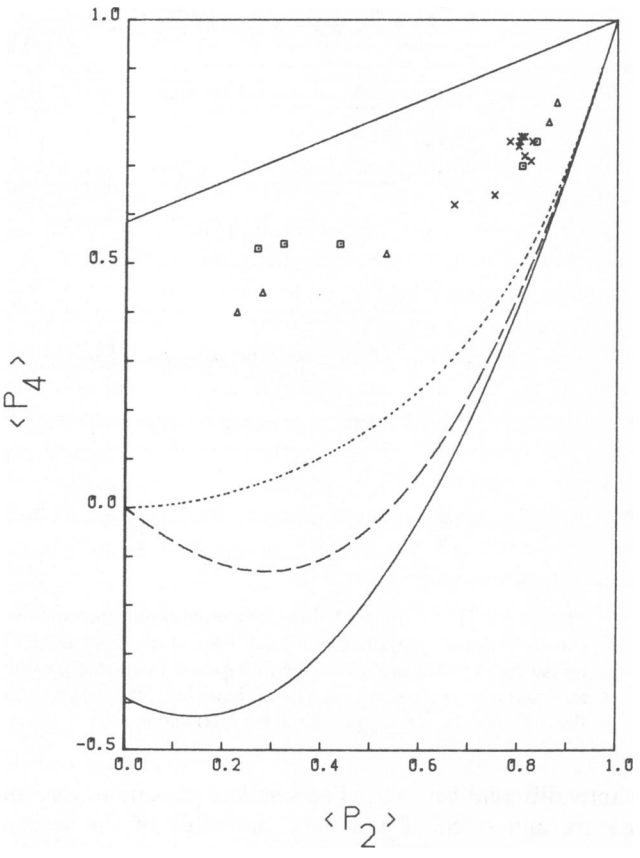

FIGURE 3 The $\langle P_2 \rangle \langle P_4 \rangle$ plane with the obtained order parameter values for DPH in vesicles of DMPC (△) and DPPC (□) and in DMPC/α-lactalbumin complexes (x). The solid lines in the plane indicate the theoretical upper and lower limits. For comparison, the relation between $\langle P_2 \rangle$ and $\langle P_4 \rangle$ is also shown for the cone model (---) and the Gaussian model (· · ·).

TABLE VI

VALUES OF THE ROTATIONAL DIFFUSION CONSTANT $D_\perp$ FOR THE VARIOUS DESCRIPTIONS OF THE FLUORESCENCE ANISOTROPY OF DPH IN UNILAMELLAR VESICLES OF DMPC AND DPPC (VALUES FOR $\langle P_2 \rangle$ AND $\langle P_4 \rangle$ ARE ALSO GIVEN FOR THE r_{g3} MODEL)

Sample	T(°C)	r_{c1} $D_\perp$	r_{g1} $D_\perp$	r_{c3} $D_\perp$	r_{gc} $D_\perp$	r_{g3}			r_{m2} $D_\perp$
						$D_\perp$	$\langle P_2 \rangle$	$\langle P_4 \rangle$	
		ns^{-1}	ns^{-1}	ns^{-1}	ns^{-1}	ns^{-1}			ns^{-1}
DMPC	7.7	0.0151	0.012	0.015	0.0134	0.04	0.877	0.83	0.03
		(0.0009)*	(0.001)	(0.001)	(0.0009)	(0.02)	(0.006)	(0.03)	(0.01)
	16.3	0.035	0.027	0.034	0.031	0.08	0.859	0.79	0.08
		(0.003)	(0.002)	(0.003)	(0.002)	(0.08)	(0.003)	(0.06)	(0.04)
	24.3	0.082	0.059	0.077	0.075	0.12	0.529	0.52	0.10
		(0.002)	(0.002)	(0.002)	(0.002)	(0.02)	(0.006)	(0.03)	(0.01)
	35.4	0.172	0.113	0.159	0.136	0.26	0.278	0.44	0.20
		(0.003)	(0.002)	(0.002)	(0.002)	(0.03)	(0.005)	(0.02)	(0.02)
	42.0	0.238	0.155	0.221	0.180	0.33	0.227	0.40	0.28
		(0.004)	(0.003)	(0.004)	(0.003)	(0.05)	(0.006)	(0.03)	(0.04)
DPCC	22.3	0.047	0.038	0.046	0.043	0.09	0.835	0.75	0.1
		(0.03)	(0.003)	(0.003)	(0.003)	(0.06)	(0.003)	(0.05)	(0.2)
	32.4	0.070	0.056	0.069	0.065	0.2	0.806	0.7	0.14
		(0.004)	(0.003)	(0.004)	(0.004)	(0.2)	(0.003)	(0.1)	(0.08)
	40.3	0.159	0.110	0.150	0.141	0.3	0.436	0.54	0.21
		(0.004)	(0.003)	(0.004)	(0.003)	(0.2)	(0.004)	(0.08)	(0.03)
	45.4	0.224	0.149	0.209	0.184	(0.6)	0.321	0.54	0.27
		(0.005)	(0.004)	(0.005)	(0.005)	(0.3)	(0.005)	(0.07)	(0.03)
	51.8	0.288	0.188	0.270	0.225	0.8	0.268	0.53	0.4
		(0.007)	(0.005)	(0.006)	(0.006)	(0.5)	(0.006)	(0.07)	(0.1)

*Standard deviations are denoted within parentheses.

in the χ_r^2 values with temperature for the models r_{c1}, r_{c3}, and r_{gc} (see Table V). The consequences of the observed $\langle P_2 \rangle \langle P_4 \rangle$ relation will be discussed in the next section.

The value of the rotational diffusion coefficent $D_\perp$ is strongly influenced by the underlying model (see Table VI). Note that when $D_\perp$ is not a fitting parameter, its value has to be calculated according to Eq. 10 (r_{m2}), Eq. 12 (r_{g1}), or Eq. 13 (r_{c1}). It turns out that the value of $D_\perp$ increases in the order r_{g1}, r_{c3}, r_{c1}, r_{m2}, and r_{g3}. The lower value obtained for r_{g1} as compared with r_{c1} agrees with the findings of Kinosita et al. (17). Above the transition temperature of the system, large differences between the values of $D_\perp$ for the various models exist. Note that there are relatively large uncertainties on the value of $D_\perp$ for r_{g3}. In the latter model a high correlation exists between $D_\perp$ and $\langle P_4 \rangle$, as an increase in $D_\perp$ may be compensated for by an appropriate change in $\langle P_4 \rangle$. This is not possible in the descriptions r_{c3} and r_{gc} because the independent parameters are $D_\perp$ and $\langle P_2 \rangle$, the latter being well defined. However, the behavior of the values of $D_\perp$ for r_{g3} with temperature is rather systematic. The same remarks concerning $D_\perp$ in r_{m2} can be made.

Discussion

In the preceding analysis several assumptions were made concerning the probe DPH and its behavior in vesicles. As is generally assumed, we accepted the idea that a stiff rod is a good model for the description of the dynamic behavior of DPH within the framework of the diffusion model. Attention must also be paid to the biexponential character of the total fluorescence decay. This pattern was also observed by other laboratories for isotropic media as anisotropic membranes as well (2, 3, 30, 37, 38). Reversible photoisomerization and microheterogeneity were suggested as possible explanations of this phenomenon (3, 35). However, no decisive study has been reported yet. Very recently, Cross et al. (39) treated the time-resolved polarization spectroscopy of molecules that may undergo photochemical isomerization. Their work has still to be extended to the anisotropic case. But we feel that a description that needs three rotational relaxation times on top of the two relaxations of the total fluorescence is about the current limit. In the hypothesis of microheterogeneity, each fluorescent decay component could be associated with a different anisotropy. An analysis of the data using r_{g3} then involves a very high number of adjustable parameters and has no practical value. Even by using simpler expressions, Dale et al. (3) could not obtain significant results for DPH in egg lecithin by analyzing the data towards this kind of microheterogeneity. Therefore, it seems justified to analyze the data by associating the same anisotropy to the different relaxations in the fluorescence decay (rotational homogeneity of sites).

The validity of analyzing the data with a constant value for the fundamental anisotropy, r_0, can be discussed. When the flexible description r_{m2} is used with a freely adjustable

r_0, the resulting values for r_0 are in the range (0.34, 0.40). No systematic behavior with temperature is observed. To see the effect of r_0 on the χ_r^2 value for the models r_{g3} and r_{c3}, we have analyzed the data for different values of r_0 (0.40, 0.38, 0.36, 0.34). At high order and low r_0 (0.34), the quality of the fit of r_{c3} approaches that of r_{g3}. The χ_r^2 value of the latter depends only slightly on r_0 and remains better at low order. The effect of r_0 on $\langle P_2 \rangle$ and $\langle P_4 \rangle$ as determined from r_{g3} for DPH in DPPC vesicles is shown in Fig. 4. There is only a small influence on $\langle P_2 \rangle$ but $\langle P_4 \rangle$ decreases when r_0 is lowered. The 95% confidence interval on $\langle P_4 \rangle$ has also been indicated in Fig. 4 for $r_0 = 0.380$. It may be concluded that the points $(\langle P_2 \rangle, \langle P_4 \rangle)$ deviate systematically from the $\langle P_2 \rangle \langle P_4 \rangle$ relation of the Gaussian and cone model. As a final test, the data have been analyzed by using r_{g3} for a free running r_0. Although the estimated order parameters show a large uncertainty, the results are well in line with those obtained under a fixed condition for r_0 (Fig. 4). The χ_r^2 values do not improve. Because of the deviation from the a priori models for the investigated values of r_0, we prefer to use a fixed r_0 as has been done by the originators of the cone model (1, 5).

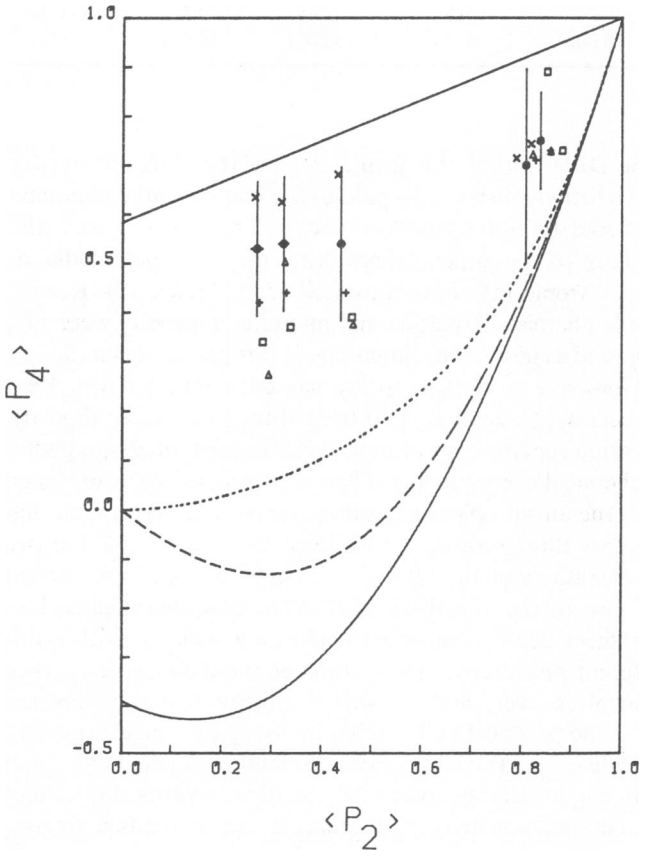

FIGURE 4 The different values of $\langle P_2 \rangle$ and $\langle P_4 \rangle$ for DPH in DPPC vesicles obtained by analyzing the data for fixed values of the fundamental anisotropy, where $r_0 = 0.400$ (×), 0.380 (○), 0.360 (+), and 0.340 (□). The results of the analyses with a free running r_0 are also indicated (△). The 95% confidence interval of $\langle P_4 \rangle$ for $r_0 = 0.380$ is marked by the vertical lines. The meaning of the other lines is given in Fig. 3.

However, instead of their value (0.395) for r_0, we take $r_0 = 0.380$ because the latter is determined on the same apparatus as used for these time-resolved experiments.

Under the mentioned conditions and restrictions, we found that the solution of the diffusion equation for anisotropic rotational motion by van der Meer et al. (8) leads to better fits than the expressions derived for the cone model. Consequently, the obtained order parameters $\langle P_2 \rangle$ and $\langle P_4 \rangle$ may expected to be reliable. The new analysis r_{g3} yields high values for $\langle P_4 \rangle$, which markedly deviate from those calculated for the cone model and the Gaussian model. Therefore, the question arises for a more appropriate distribution function. A first estimation of $f(\theta)$ may be obtained from the truncated Legendre expansion

$$f(\theta) \simeq \frac{1}{2} + \frac{5}{2} \langle P_2 \rangle P_2(\cos\theta) + \frac{9}{2} \langle P_4 \rangle P_4(\cos\theta). \quad (18)$$

For the determined order parameters, this function shows a maximum at $\theta = 0$ and $\theta = \pi/2$. Also negative values result because of the truncation. This artifact can be eliminated by the use of the information theory (40). According to this theory, $f(\theta)$ will be given by

$$f(\theta) \sim \exp [\lambda_2 P_2(\cos\theta) + \lambda_4 P_4(\cos\theta)], \quad (19)$$

where λ_2 and λ_4 are chosen in correspondence with the values $\langle P_2 \rangle$ and $\langle P_4 \rangle$. Note that in this approach a distribution function of the Gaussian type will always result when only $\langle P_2 \rangle$ can be determind from the experiment. Because the description r_{g3} allows for the independent determination of $\langle P_4 \rangle$, deviations from the Gaussian distribution may be detected. For the values obtained from $\langle P_2 \rangle$ and $\langle P_4 \rangle$ in the r_{g3} description, the maxima for $\theta = 0$ and $\theta = \pi/2$ according to Eq. 18 are confirmed (see Fig. 5). A plot of $f(\theta)\sin\theta$ vs. θ may be more interesting because the

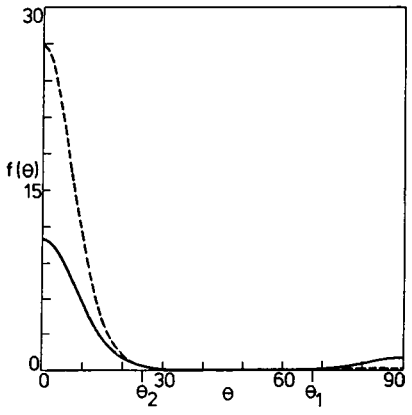

FIGURE 5 The distribution functions of the type $f(\theta) = N^{-1} \exp [\lambda_2 P_2 (\cos\theta) + \lambda_4 P_4 (\cos\theta)]$, where N is the normalization constant, for high order ($\langle P_2 \rangle = 0.860$, $\langle P_4 \rangle = 0.79$) and for low order ($\langle P_2 \rangle = 0.268$, $\langle P_4 \rangle = 0.52$), are plotted as a function of the angle θ between the symmetry axis of the DPH molecule and the membrane normal. The corresponding cone angles are also indicated: $\theta_1 = 67.3°$ for $\langle P_2 \rangle = 0.268$ (—) and $\theta_2 = 25.4°$ for $\langle P_2 \rangle = 0.860$ (---).

probability of finding the probe in a certain angular range is given by the corresponding area under the curve (see Fig. 6).

The distribution function reaches very low values in the region $40° < \theta < 60°$. Hence two fractions in the distribution of the probe may be distinguished. Fig. 6 clearly shows that for low order the fractions of the probe in the plane and perpendicular to the membrane may become nearly equal. This explains why the unimodal distributions corresponding to the cone model and the Gaussian model are not appropriate at $T > T_c$. The fraction α corresponding to the distribution peak around $\theta = 0$ vs. $\langle P_2 \rangle$ is represented in Fig. 7. This implies a different interpretation of the limiting anisotropy as reflected by DPH. The lower values of $\langle P_2 \rangle$ for $T > T_c$ have usually been interpreted in terms of a larger cone angle and in less organization of the surrounding lipids. This idea should be taken very cautiously. Indeed, the order of the acyl chain as probed by the DPH molecules along the normal to the bilayer may still be reasonably high because a population of the probes $\theta = \pi/2$ tends to decrease the value of $\langle P_2 \rangle$. Note that when the angle between the directions of the symmetry axis of the probe at the times of absorption and emission is larger than the magic angle of 54.7°, this will result in a negative contribution to the overall anisotropy. In this context, the gel-to-liquid transition of the vesicle system, as probed by DPH, may be seen as a shift in the dynamic equilibrium of DPH between the orientations perpendicular to and parallel with the plane of the membrane. This explains why the anisotropy of DPH shows such a drastic change around the transition temperature. This depolarization by the motion of DPH towards the plane in the middle of the bilayer has already been suggested by Engel et al. (41).

Recently, charged derivatives of DPH were introduced as fluorescent probes of lipid bilayers (42, 43). The cationic analogue TMA-DPH is thought to be anchored at the lipid-water interface with the DPH moiety intercalated between the upper portions of the fatty acyl chains. This model has been supported by the high $r(\infty)$ value for TMA-DPH as compared with DPH for $T > T_c$ (41). So

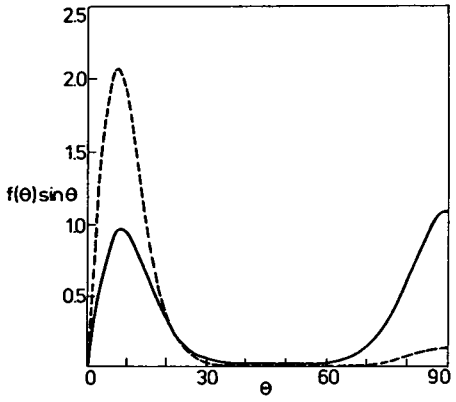

FIGURE 6 $f(\theta)\sin\theta$ as a function of θ for the same values of $\langle P_2 \rangle$ and $\langle P_4 \rangle$ as in Fig. 5: $\langle P_2 \rangle = 0.268$ (—) and $\langle P_4 \rangle = 0.86$ (---).

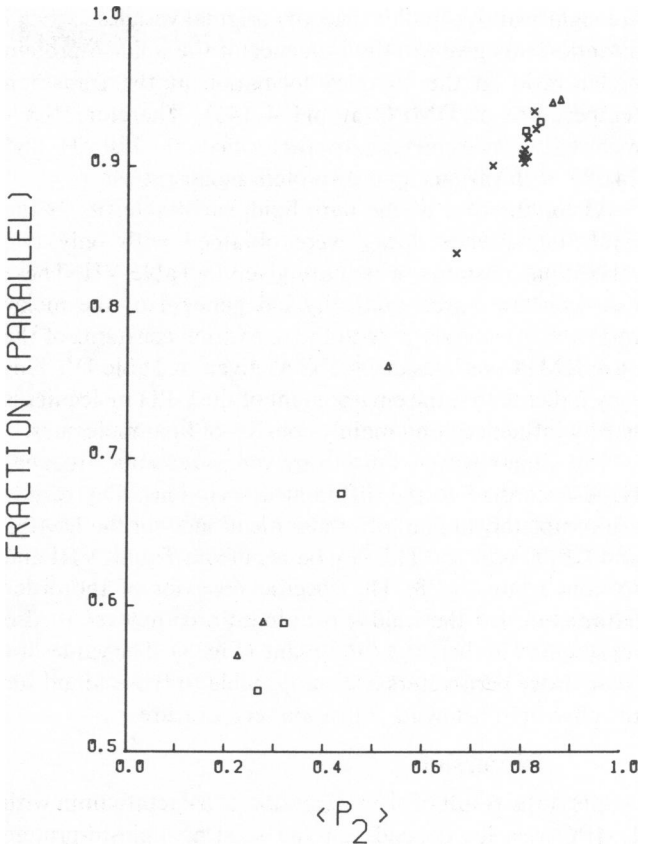

FIGURE 7 The fraction α of the DPH probes having their long axis parallel to the normal on the membrane for DPH in vesicles of DMPC (△) and DPPC (□) and in DMPC/α-lactalbumin complexes (×).

the motion of TMA-DPH might be described by a cone with the top at the head group of the phospholipids. Our preliminary results on TMA-DPH in DPPC showed that the cone interpretation, r_{gc}, resulted in a perfect fit above and below T_c. The fact that the quality of the fit is even better than for DPH with $r_{gc}(t)$ may suggest that the motion of the latter is far more complex than that for TMA-DPH. Note, however, that adequate fits of the total fluorescence of TMA-DPH in DPPC require at least two relaxation constants.

THE TIME-DEPENDENT FLUORESCENCE ANISOTROPY OF DPH IN DMPC/α-LACTALBUMIN COMPLEXES

Results

To investigate whether the deviation from the Gaussian and the cone model also appears in other systems, we measured the time-resolved anisotropy of DPH embedded in complexes of DMPC and α-lactalbumin. This system has already been studied extensively (44–47). In summary, at physiological pH α-lactalbumin adsorbs only to the outer surface of the vesicles. At pH 4, however, it has an apolipoprotein-like behavior; it interacts with the apolar phase of phosphatidylcholine vesicles to form particles that

are significantly smaller than the original vesicles. Special attention was given to the influence of the lipid-to-protein molar ratio on the complex formation at the transition temperature of DMPC at pH 4 (46). Therefore time-resolved measurements are performed at this pH and 24.2°C with various lipid-to-protein molar ratios.

As for the case of the pure lipid, satisfiable fits of the total fluorescence decay were obtained with only two relaxation constants, which are given in Table VII. These time constants are practically independent of the molar ratio and are comparable to the relaxation constants of the pure DMPC vesicles at 24.2°C as given in Table IV. This may indicate that the environment of the DPH molecules is hardly influenced and mainly consists of lipid molecules.

The time-resolved anisotropy measurements are analyzed according to the different descriptions. The results are completely in line with those mentioned for the DMPC and DPPC vesicles. This can be seen from Tables VIII and IX and from Fig. 8. The specific behavior of the order parameters for the lipid-α-lactalbumin complexes is also represented in the $\langle P_2 \rangle \langle P_4 \rangle$ plane (Fig. 3). The values for these order parameters are comparable to those found for the pure lipid below its transition temperature.

Discussion

At pH 4 the result of the interaction of α-lactalbumin with DMPC vesicles depends on the starting lipid-to-protein molar ratio (46). At 24°C and for molar ratios ~170, the vesicles begin to disrupt and lipid-protein complexes with a lipid-to-protein molar ratio of ~70:1 are formed. For starting molar ratios <70, all the vesicles are disrupted. The time-resolved anisotropy analysis demonstrates that

TABLE VII

THE DECAY PARAMETERS FOR THE TOTAL FLUORESCENCE EMISSION, $s(t)$, OF DPH IN LIPID-α-LACTALBUMIN COMPLEXES, AS A FUNCTION OF THE LIPID-TO-PROTEIN MOLAR RATIO, AT 24.2°C AND AT pH 4

Molar ratio	a_1	a_2	τ_1	τ_2
			ns	*ns*
10	0.126	0.874	3.0	10.50
	(0.006)*	(0.006)	(0.3)	(0.03)
29	0.142	0.858	3.4	10.63
	(0.007)	(0.007)	(0.3)	(0.04)
52	0.18	0.82	4.2	10.57
	(0.01)	(0.01)	(0.3)	(0.05)
60	0.147	0.853	3.0	10.70
	(0.005)	(0.005)	(0.2)	(0.03)
83	0.144	0.856	2.6	10.63
	(0.005)	(0.005)	(0.2)	(0.03)
88	0.140	0.860	3.7	10.62
	(0.008)	(0.008)	(0.3)	(0.04)
93	0.121	0.879	3.0	10.45
	(0.006)	(0.006)	(0.3)	(0.03)
153	0.159	0.842	3.7	10.67
	(0.008)	(0.008)	(0.3)	(0.04)
200	0.18	0.82	4.0	10.57
	(0.01)	(0.01)	(0.3)	(0.05)
644	0.190	0.840	3.3	9.86
	(0.008)	(0.008)	(0.2)	(0.04)

Different amounts of a 24-mg/ml α-lactalbumin solution were incubated with 3 ml vesicles that were at a concentration of ≈0.8 mg/ml.
*Standard deviations are denoted within parentheses.

TABLE VIII

THE QUALITY OF THE FITS AS JUDGED BY THE REDUCED CHI SQUARE VALUE, χ_r^2*, ACCORDING TO THE VARIOUS DESCRIPTIONS OF THE FLUORESCENCE ANISOTROPY FOR DPH IN DMPC/α-LACTALBUMIN COMPLEXES AT pH 4 AND AT 24.2°C.

Molar ratio	r_{c1} r_{g1}	r_{c3}	r_{gc}	r_{g3}	r_{m2}
10	1.41	1.39	1.39	1.19	1.19
29	1.68	1.64	1.63	1.24	1.23
52	1.48	1.43	1.42	1.03	1.01
60	1.69	1.65	1.65	1.34	1.32
83	1.33	1.31	1.30	1.13	1.13
88	1.17	1.15	1.15	1.05	1.05
93	1.30	1.26	1.26	1.07	1.08
153	1.35	1.32	1.32	1.06	1.04
200	1.20	1.16	1.15	1.02	1.02
644	1.41	1.33	1.32	1.08	1.07

*See Eq. 17.

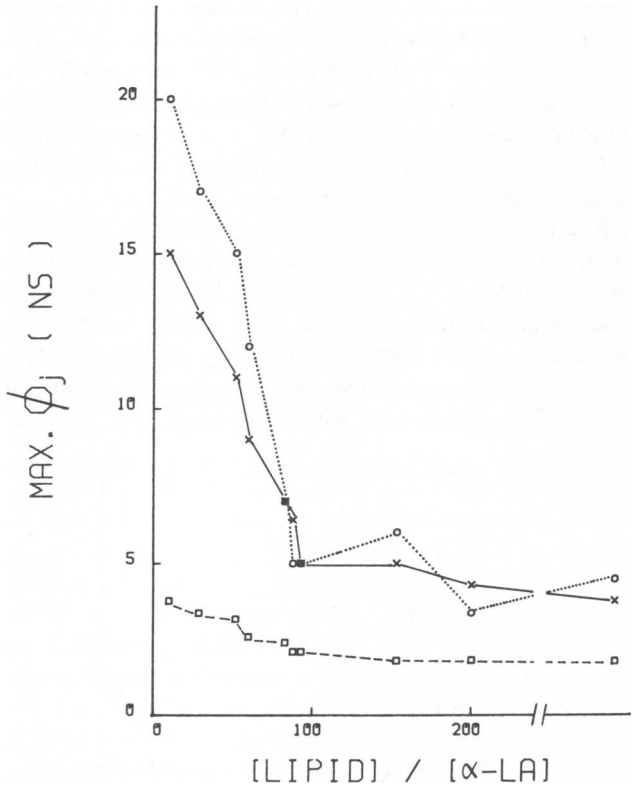

FIGURE 8 The largest relaxation time in the expressions of the fluorescence anisotropy according to the descriptions r_{m2} (t) (· O ·), $r_{c3}(t)$ (–□–) and $r_{g3}(t)$ (–X–) as obtained from the experiments on DPH in DMPC/α-lactalbumin complexes as a function of the lipid-to-protein molar ratio. The highest value of this ratio is 644.

TABLE IX

VALUES OF THE ROTATIONAL DIFFUSION CONSTANT $D_\perp$ FOR THE VARIOUS DESCRIPTIONS OF THE FLUORESCENCE ANISOTROPY OF DPH IN LIPID-α-LACTALBUMIN COMPLEXES AS A FUNCTION OF THE MOLAR RATIO AT pH 4 AND AT 24.2°C (VALUES FOR $\langle P_2 \rangle$ AND $\langle P_4 \rangle$ ARE ALSO GIVEN FOR THE r_{g3} MODEL)

Molar ratio	r_{c1} $D_\perp$	r_{g1} $D_\perp$	r_{c3} $D_\perp$	r_{gc} $D_\perp$	r_{g3}			r_{m2} $D_\perp$
					$D_\perp$	$\langle P_2 \rangle$	$\langle P_4 \rangle$	
	ns^{-1}	ns^{-1}	ns^{-1}	ns^{-1}	ns^{-1}			ns^{-1}
10	0.0189	0.0151	0.0182	0.0169	0.035	0.801	0.75	0.028
	(0.0003)*	(0.0003)	(0.0009)	(0.0008)	(0.017)	(0.009)	(0.04)	(0.005)
29	0.0193	0.0155	0.0187	0.0173	0.038	0.810	0.76	0.030
	(0.0008)	(0.0007)	(0.0009)	(0.0008)	(0.013)	(0.006)	(0.03)	(0.004)
52	0.223	0.0178	0.0216	0.0201	0.045	0.803	0.76	0.036
	(0.0009)	(0.0008)	(0.0009)	(0.0009)	(0.015)	(0.005)	(0.03)	(0.005)
60	0.025	0.020	0.024	0.022	0.043	0.827	0.75	0.036
	(0.001)	(0.001)	(0.001)	(0.001)	(0.013)	(0.004)	(0.03)	(0.005)
83	0.031	0.025	0.030	0.028	0.050	0.810	0.72	0.045
	(0.001)	(0.001)	(0.001)	(0.001)	(0.013)	(0.004)	(0.03)	(0.009)
88	0.032	0.026	0.031	0.029	0.043	0.823	0.71	0.042
	(0.001)	(0.001)	(0.001)	(0.001)	(0.007)	(0.003)	(0.02)	(0.008)
93	0.038	0.030	0.037	0.035	0.084	0.798	0.74	0.069
	(0.002)	(0.001)	(0.002)	(0.002)	(0.051)	(0.003)	(0.06)	(0.021)
153	0.042	0.034	0.041	0.039	0.101	0.801	0.75	0.098
	(0.002)	(0.002)	(0.002)	(0.002)	(0.093)	(0.003)	(0.08)	(0.035)
200	0.056	0.044	0.055	0.052	0.082	0.749	0.64	0.085
	(0.002)	(0.002)	(0.002)	(0.002)	(0.016)	(0.003)	(0.03)	(0.022)
644	0.078	0.059	0.075	0.073	0.139	0.667	0.62	0.107
	(0.003)	(0.002)	(0.003)	(0.003)	(0.056)	(0.003)	(0.06)	(0.017)
∞	0.082	0.059	0.077	0.075	0.12	0.529	0.52	0.10
	(0.002)	(0.002)	(0.002)	(0.002)	(0.02)	(0.006)	(0.03)	(0.01)

*Standard deviations are denoted within parentheses.

the protein has an effect on the dynamics of the DPH probe as well as on the structure of the environment for all the molar ratios used in these experiments. Under the influence of α-lactalbumin the order parameters $\langle P_2 \rangle$ and $\langle P_4 \rangle$ increase. As for the discussed vesicles systems, the rotational correlation times increase with increasing order (Fig. 8). When all the vesicles are disrupted (at low molar ratios), a highly ordered lipoprotein complex is obtained. In this case ~90–95% of the DPH molecules are aligned parallel to the acyl chains of the phospholipids (Fig. 7). Even at high molar ratio ($N = 644$) when the vesicles are not disrupted, α-lactalbumin has a strong ordering effect: $\langle P_2 \rangle$ increased from 0.529 to 0.667 (26%) and $\langle P_4 \rangle$ increased from 0.52 to 0.62 (19%). This agrees with the fact that molar ratios of >170, α-lactalbumin strongly associates with the vesicles (46). At molar ratios 80–90, when all the vesicles are disrupted, there is a drastic decrease of $D_\perp$ (Table IX). At the same time the different rotational correlation times dramatically increase, especially the largest one.

A remark concerning the values of the ϕ_j's must be made. As the protein is able to disrupt the vesicles and to form smaller particles, the question arises if the rotating lipoprotein complex itself contributes to the measured correlation times. From the electron micrograph shown in reference 44 it is supposed that the complex has the shape of a prolate ellipsoid of revolution with an axial ratio of 3.3. According to Tao (48), the rotation of the macromolecule must be described by means of three correlation times. Following his method, the following relaxation times for the complex at 24°C were calculated: $\phi_1 \simeq 900$ ns, $\phi_2 \simeq 600$ ns and $\phi_3 \simeq 300$ ns. These values are too high to be detected in our experiments, and the measured ϕ_j's describe the rotational relaxation of DPH in the complex. In the calculations a viscosity of 0.9111 cP was assumed (49). The volume of the complex itself was about 1.6×10^{-18} cm^3, calculated from its molar mass M and its partial specific volume $\bar{v}$: $M = (1.05 \pm 0.16)\ 10^6$ g/mol and $\bar{v} = 0.19 \pm 0.01$ cm^3/g (46).

CONCLUSION

The application of the general approach to the analysis of time-dependent anisotropy measurements (8) leads to a reliable estimation of the order parameters $\langle P_2 \rangle$ and $\langle P_4 \rangle$ of the distribution of the fluorescent probe in membrane suspensions. For DPH in vesicles of DMPC or DPPC and in DMPC/α-lactalbumin complexes the experimentally found relations between $\langle P_2 \rangle$ and $\langle P_4 \rangle$ are very similar and deviate from those predicted by the cone and the Gaussian model.

An orientational distribution function of the probe may then be estimated from an information theoretic approach (40). It turns out that orientational distributions with only one maximum (e.g., the cone and the Gaussian distribu-

tion) are not suited for the description of the behavior of DPH in the systems investigated in this report.

The results indicate that a fraction of the probe molecules is oriented parallel to the preferred direction of the lipids and that the remaining fraction is oriented perpendicular to this direction. In the pure lipid systems, the latter contribution is small below T_c but above T_c the two fractions are nearly equal. Also in the lipid protein complexes, two fractions of the probe molecules along mutual perpendicular directions can be distinguished.

The interpretation of the limiting anisotropy $r(\infty)$ of DPH towards the organization of its microenvironment is not straightforward. Fluorescent analogues of DPH (e.g., TMA-DPH and DPH-phosphatidylcholine [50]) may be used to shed more light on this relation because the position of the probe in the system may be known more accurately.

APPENDIX A

It has been shown (6, 7) that the distribution function $f(\theta)$ can be expanded in the complete set of orthogonal Legendre polynomials P_{2l} (cos θ):

$$f(\theta) = \sum_{l=0}^{\infty} \frac{4l+1}{2} \langle P_{2l} \rangle P_{2l}(\cos\theta)$$

where

$$\langle P_{2l} \rangle = \int_0^{\pi} P_{2l}(\cos\theta) f(\theta) \sin\theta d\theta.$$

The first Legendre polynomials of even rank are given by

$$P_2(\cos\theta) = \tfrac{1}{2}(3\cos^2\theta - 1)$$

$$P_4(\cos\theta) = \tfrac{1}{8}(35\cos^4\theta - 30\cos^2\theta + 3).$$

The second- and fourth-rank order parameters corresponding to the cone model (5) with an angle θ_c are

$$\langle P_2 \rangle = \tfrac{1}{2}\cos\theta_c(1 + \cos\theta_c)$$

$$\langle P_4 \rangle = \tfrac{1}{8}\cos\theta_c(1 + \cos\theta_c)(7\cos^2\theta_c - 3).$$

APPENDIX B

The time-dependent anisotropy $r(t)$ can be expressed in terms of a correlation function (5, 8, 9, 10) as

$$r(t)/r(0) = \ll P_2(\mu_0 \cdot \mu_t) \gg \qquad \text{(B1)}$$

where μ denotes a unit vector along the symmetry axis of the rod shaped probe, and where subscripts are used for the time indication. It is assumed that at least one optical transition moment has the direction of μ. By applying the addition theorem for spherical harmonics, Eq. B1 can be written as

$$r(t)/r(0) = \sum_{k=-2}^{2} G_{k0}(t),$$

with

$$G_{00}(t) = \langle P_2(\cos\theta_0) P_2(\cos\theta_t) \rangle$$

$$G_{10} = G_{-10} = \tfrac{3}{2}\langle \sin\theta_0 \cos\theta_0 \sin\theta_t \cos\theta_t \cos(\phi_0 - \phi_t) \rangle$$

$$G_{20} = G_{-20} = \tfrac{3}{8}\langle \sin^2\theta_0 \sin^2\theta_t \cos 2(\phi_0 - \phi_t) \rangle,$$

where θ_t, ϕ_t are the polar and the azimuthal angle of μ at time t.

Thanks are due to Dr. R. Todesco (Limburgs Universitair Centrum, Diepenbeek) for checking the purity of DPH on HPLC and to Mrs. G. Dewitte and N. Holvoet (Katholieke Universiteit Leuven, campus Kortrijk) for technical assistance.

W. van der Meer is supported by the Koningin Wilhelmina Fonds, the Netherlands Cancer Foundation. This study was supported by a grant of the National Fonds voor Wetenschappelijk Onderzoek.

Received for publication 2 November 1983 and in final form 24 April 1984.

REFERENCES

1. Kawato, S., K. Kinosita, Jr., and A. Ikegami. 1977. Dynamic structure of lipid bilayers studied by nanosecond fluorescence techniques. *Biochemistry.* 16:2319–2324.
2. Chen, L. A., R. E. Dale, S. Roth, and L. Brand. 1977. Nanosecond time-dependent fluorescence depolarization of diphenylhexatriene in dimyristoyl-lecithin vesicles and the determination of "microviscosity." *J. Biol. Chem.* 252:2163–2169.
3. Dale, R. E., L. A. Chen, and L. Brand. 1977. Rotational relaxation of the microviscosity probe diphenylhexatriene in paraffin oil and egg lecithin vesicles. *J. Biol. Chem.* 252:7500–7510.
4. Lakowicz, J. R., and F. G. Prendergast. 1978. Quantitation of hindered rotation of diphenylhexatriene in lipid bilayers by differential polarized phase fluorometry. *Science (Wash. DC).* 200:1399–1401.
5. Kinosita, K., Jr., S. Kawato, and A. Ikegami. 1977. A theory of fluorescence polarization decay in membranes. *Biophys. J.* 20:289–305.
6. Heyn, M. P. 1979. Determination of lipid order parameters and rotational correlation times for fluorescence polarization experiments. *FEBS (Fed. Eur. Biochem. Soc.) Lett.* 108:359–364.
7. Jähnig, F. 1979. Structural order of lipids and proteins in membranes: evaluation of fluorescence anisotropy data. *Proc. Natl. Acad. Sci. USA.* 76:6361–6365.
8. Van der Meer, W., H. Pottel, W. Herreman, M. Ameloot, H. Hendrickx, and H. Schröder. 1984. Effect of orientational order on the decay of the fluorescence anisotropy in membrane suspensions. A new approximate solution of the rotational diffusion equation. *Biophys. J.* 46:515–523.
9. Lipari, G., and A. Szabo. 1980. Effect of librational motion on fluorescence depolarization and nuclear magnetic resonance relaxation in macromolecules and membranes. *Biophys. J.* 30:489–506.
10. Lipari, G., and A. Szabo. 1981. Padé approximants to correlation functions for restricted rotational diffusion. *J. Chem. Phys.* 75:2971–2976.
11. Badea, M. G., and L. Brand. 1979. *Methods Enzymol.* 61:378–425.
12. Cundall, R. B., and R. E. Dale, editors. NATO Advanced Study Institute: Time-Resolved Fluorescence Spectroscopy in Biochemistry and Biology. Plenum Publishing Corp., New York.
13. Bouchy, M., editor. 1982. Conference proceedings, Nancy, France. *In* Deconvolution and Reconvolution. Ecole Nationale Superieure des Industries Chimiques de l'Institut Nationale Polytechnique de Lorraine, France.
14. Ameloot, M., and H. Hendrickx. 1982. Criteria for model evaluation in the case of deconvolution calculations. *J. Chem. Phys.* 76:4419–4432.
15. Wahl, Ph. 1979. Analysis of fluorescence anisotropy decays by a least squares method. *Biophys. Chem.* 10:91–104.
16. Dale, R. E. 1983. Time-Resolved Fluorescence Spectroscopy in Biochemistry and Biology. R. B. Cundall and R. E. Dale, editors. Plenum Publishing Corp., New York. 605–612.
17. Kinosita, K., Jr., A. Ikegami, and S. Kawato. 1982. On the wobbling-in-cone analysis of fluorescence anisotropy decay. *Biophys. J.* 37:461–464.
18. Ameloot, M., and H. Hendrickx. 1983. Extension of the performance

of Laplace deconvolution in the analysis of fluorescence decay curves. *Biophys. J.* 44:27–38.

19. André, J. C., M. Bouchy, J. L. Viovy, L. M. Vincent, and B. Valeur. 1982. Use of regularization operators together with Lagrange multipliers in numerical deconvolution of flourescence decay curves. *Comput. & Chem.* 6:5–13.
20. Zannoni, C., A. Arcioni, and P. Cavatorta. 1983. Fluorescence depolarization in liquid crystals and membrane layers. *Chem. Phys. Lipids.* 32:179–250.
21. Nordio, P. L., and U. Segre. 1979. Rotational dynamics. *In* The Molecular Physics of Liquid Crystals. G. R. Luckhurst and G. W. Gray, editors. Academic Press, London. 411–426.
22. Böhlen, P., S. Stein, W. Dairman, and S. Udenfriend. 1973. Fluorometric assay of proteins in the nanogram range. *Arch. Biochem. Biophys.* 155:213–220.
23. Vaskovsky, V. E., E. Y. Kostetsky, and I. M. Vasendin. 1975. A universal reagent for phospholipid analysis. *J. Chromatogr.* 114:129–141.
24. Hazan, G. H., A. Grinvald, M. Maytal, and I. Z. Steinberg. 1974. An improvement of nanosecond fluorimeters to overcome drift problems. *Rev. Sci. Instrum.* 45:1602–1604.
25. Chen, R. F., and R. L. Bowman. 1965. Fluorescence polarization: measurement with ultraviolet-polarizing filters in a spectrophotofluorometer. *Science (Wash. DC).* 147:729–732.
26. Grinvald, A., and I. Z. Steinberg. 1974. On the analysis of fluorescence decay kinetics by the method of least squares. *Anal. Biochem.* 59:583–598.
27. Marquardt, D. W. 1963. An algorithm for least-squares estimation of nonlinear parameters. *J. Soc. Ind. Appl. Math.* 11:431–441.
28. Grinvald, A. 1976. The use of standards in the analysis of fluorescence decay data. *Anal. Biochem.* 75:260–280.
29. Bevington, Ph. R. 1969. Data Reduction and Error Analysis for the Physical Sciences. McGraw-Hill, Inc., New York.
30. Stubbs, C. D., T. Kouyama, K. Kinosita, and A. Ikegami. 1981. Effect of double bonds on the dynamic properties of hydrocarbon region of lecithin bilayers. *Biochemistry.* 20:4257–4262.
31. Van Blitterswijk, W. J., R. P. Van Hoeven, and B. W. van der Meer. 1981. Lipid structural order parameters (reciprocal of fluidity) in biomembranes derived from steady-state fluorescence polarization measurements. *Biochim. Biophys. Acta.* 644:323–332.
32. Pottel, H., W. van der Meer, and W. Herreman. 1983. Correlation between the order parameter and the steady-state fluorescence anisotropy of 1,6-diphenyl-1,3,5-hexatriene and an evaluation of membrane fluidity. *Biochim. Biophys. Acta.* 730:181–186.
33. Hare, F. 1983. Simplified derivation of angular order and dynamics of rodlike fluorophores in models and membranes. Simultaneous estimation of the order and fluidity parameters for diphenylhexatriene by only coupling steady-state illumination polarization and lifetime of fluorescence. *Biophys. J.* 42:205–218.
34. Wolber, P. K., and B. S. Hudson. 1981. Fluorescence lifetime and time-resolved polarization anisotropy studies of acyl chain order and dynamics in lipid bilayers. *Biochemistry.* 20:2800–2810.
35. Shinitzky, M., and Y. Barenholz. 1974. Dynamics of the hydrocarbon layer in liposomes of lecithin sphingomyelin containing dicetylphosphate. *J. Biol. Chem.* 249:2652–2657.
36. Hare, F., and C. Lussan. 1977. Variations in microviscosity values induced by different rotational behaviour of fluorescent probes in some aliphatic environments. *Biochim. Biophys. Acta.* 467:262–272.
37. Kinosita, K., Jr., S. Kawato, A. Ikegami, S. Yoshida, and Y. Orii. 1981. The effect of cytochrome oxidase on lipid chain dynamics. A nanosecond fluorescence depolarization study. *Biochim. Biophys. Acta.* 647:7–17.
38. Birch, D. J. S., and R. E. Imhof. 1977. A single photon-counting fluorescence decay-time spectrometer. *J. Physics E.* 10:1044–1049.
39. Cross, A. J., D. H. Waldeck, and G. R. Fleming. 1983. Time resolved polarization spectroscopy: level kinetics and rotational diffusion. *J. Chem. Phys.* 78:6455–6467.
40. Berne, B. J., P. Pechukas, and G. D. Harp. 1968. Molecular reorientation in liquids and gases. *J. Chem. Phys.* 49:3125–3129.
41. Engel, L. W., and F. G. Prendergast. 1981. Values for and significance of order parameters and "cone angles" of fluorophore rotation in lipid bilayers. *Biochemistry.* 20:7338–7345.
42. Cundall, R. B., I. Johnson, M. W. Jones, E. W. Thomas, and I. H. Munro. 1979. Photophysical properties of DPH derivatives. *Chem. Phys. Lett.* 64:39–42.
43. Prendergast, F. G., R. P. Haugland, and P. J. Callahan. 1981. 1-[4-(Trimethylamino)phenyl]-6-phenylhexa-1,3,5-triene: synthesis, fluorescence properties, and use as a fluorescence probe of lipid bilayers. *Biochemistry.* 20:7333–7338.
44. Hanssens, I., C. Houthuys, W. Herreman, and F. H. Van Cauwelaert. 1980. Interaction of α-lactalbumin with dimyristoylphosphatidylcholine vesicles. I. A microcalorimetric and fluorescence study. *Biochim. Biophys. Acta.* 602:539–557.
45. Herreman, W., Ph. Van Tornout, F. H. Van Cauwelaert, and I. Hanssens. 1981. Interaction of α-lactalbumin with dimyristoylphosphatidylcholine vesicles. II. A fluorescence polarization study. *Biochim. Biophys. Acta.* 640:419–429.
46. Hanssens, I., W. Herreman, J.-C. Van Ceunebroeck, H. Dangreau, C. Gielens, G. Preaux, and F. H. Van Cauwelaert. 1983. Interaction of α-lactalbumin with dimyristoylphosphatidylcholine vesicles. III. Influence of the temperature and of the lipid-to-protein molar ratio on the complex formation. *Biochim. Biophys. Acta.* 728:293–304.
47. Van Cauwelaert, F. H., I. Hanssens, W. Herreman, J. -C. Van Ceunebroeck, J. Baert, and H. Berghmans. 1983. Comparison of the enthalpy state of vesicles of different size by their interaction with α-lactalbumin. *Biochim. Biophys. Acta.* 727:273–284.
48. Tao, T. 1969. Time-dependent fluorescence depolarization and Brownian diffusion coefficients of macromolecules. *Biopolymers.* 8:609–632.
49. Weast, R. C. 1973. Handbook of Chemistry and Physics. The Chemical Rubber Comp., Cleveland, OH. 53 ed. F36.
50. Morgan, C. G., E. W. Thomas, T. S. Moras, and Y. P. Yianini. 1982. The use of a phospholipid analogue of diphenyl-1,3,5-hexatriene to study melittin-induced fusion of small unilamellar phospholipid vesicles. *Biochim. Biophys. Acta.* 692:196–201.